Check for updates

AGU ADVANCING EARTH AND SPACE SCIENCE

Geophysical Research Letters

RESEARCH LETTER
10.1029/2020GL087357

C. W. and Z. H. contributed equally.

Key Points:
- Reservoir construction changed the transport process and deposition pattern of organic carbon in the East China Sea
- The deposition flux of organic carbon in the East China Sea decreased by 48% due to reservoir construction
- Deposition flux reduction threatens river-dominated margins worldwide and should be taken seriously

Supporting Information:
- Supporting Information S1

Correspondence to:
X. Zou,
zouxq@nju.edu.cn

Citation:
Wang, C., Hao, Z., Gao, J., Feng, Z., Ding, Y., Zhang, C., & Zou, X. (2020). Reservoir construction has reduced organic carbon deposition in the East China Sea by half since 2006. *Geophysical Research Letters*, *47*, e2020GL087357. https://doi.org/10.1029/2020GL087357

Received 3 FEB 2020
Accepted 17 AUG 2020
Accepted article online 21 AUG 2020

©2020. American Geophysical Union. All Rights Reserved.

Reservoir Construction Has Reduced Organic Carbon Deposition in the East China Sea by Half Since 2006

Chenglong Wang[1], Zhe Hao[2,3], Jianhua Gao[1], Ziyue Feng[1], Yongcheng Ding[1], Chuchu Zhang[1], and Xinqing Zou[1,2]

[1]School of Geographic and Oceanographic Sciences, Ministry of Education Key Laboratory for Coast and Island Development, Nanjing University, Nanjing, China, [2]Collaborative Innovation Center of South China Sea Studies, Nanjing University, Nanjing, China, [3]Key Laboratory of Engineering Oceanography, Second Institute of Oceanography, Ministry of Natural Resources, Hangzhou, China

Abstract River-dominated marginal seas are important carbon sinks on Earth. However, their carbon sequestration capacities are changing due to increased anthropogenic perturbations. Herein, we employ substantial datasets to study the characteristics of organic carbon (OC) from the East China Sea (ECS) in 2006 and 2018 and reveal the impacts of reservoir construction on the OC deposition in this region. We show that the distribution of sedimentary OC in the ECS is primarily controlled by riverine input and seabed erosion processes. Hydrodynamic processes influence the OC deposition due to both the scouring of fine-grained sediments and selective degradation of OC associated with the sediment mobilization. The deposition flux of OC in the ECS decreased by 48% after reservoir construction. These findings demonstrate that reservoir construction seriously affected the OC deposition in the ECS and may be applicable to river-dominated continental shelves worldwide.

1. Introduction

Approximately 87% of the land surface is linked to oceans by rivers (Ludwig & Probst, 1998), which annually export ~200 Mt of terrestrial particulate organic carbon (POC) to marginal seas (Galy et al., 2015). In addition, marginal seas are characterized by high primary productivities due to high nutrient inputs from the continent. Therefore, marginal seas are considered major locations of organic carbon (OC) burial and are known to have ~80% of the buried OC in global oceans (Burdige, 2005). Over the last 50 years, source-to-sink sedimentary systems, primary locations of OC transport and burial, have been drastically perturbed by human activities (Bröder et al., 2018; Raymond et al., 2007). For example, reservoir construction intercepts large amounts of sediment, which directly reduces POC flux (Bianchi & Allison, 2009; Li et al., 2015) and changes the delta and adjacent continental shelf environments (Blum & Roberts, 2009; Gao et al., 2019). Therefore, river-dominated marginal seas are in a systemic regime shift, and attention should be paid to the effects of this shift on the OC burial.

The Changjiang-East China Sea (ECS) is a typical source-to-sink sedimentary system that connects the world's longest river (i.e., the Changjiang River) with one of the widest continental shelves worldwide (i.e., the ECS continental shelf; Figure 1). The Changjiang River annually discharges ~478 Mt of sediment into the ECS (Milliman & Farnsworth, 2011) and forms the Changjiang subaqueous delta mud deposits (CSDMD) and the Zhe-Min coastal mud belt (ZMCMB) (Figure 1; Gao & Collins, 2014; Liu et al., 2007). Human activities, such as in the case of the construction of the Three Gorges Reservoir (TGR, construction of the dam began in 1994 and was not completed until 2006, impoundment began in 2003), significantly impact the transport of terrestrial materials, which further changes the sedimentary environment and biogeochemical cycles in the ECS (Gao et al., 2019; Wang, Hao, Feng, Zhang, Li, et al., 2020; Wang, Hao, Feng, Zhang, Gao, et al., 2020). In addition, the POC flux decreased from 10.9 ± 2.6 Mt yr^{-1} in the period 1952–1986 to 1.9 ± 1.0 Mt yr^{-1} in 2003–2008 (Li et al., 2015). Therefore, reservoir interception in the Changjiang River will inevitably impact the transport and burial of OC in the ECS.

In previous studies, the focus was mainly placed on the sources, composition, and distribution of OC in the ECS, and the factors affecting OC transport and deposition processes were discussed (Deng et al., 2006; Hu et al., 2012; Kao et al., 2003; Wu et al., 2013). However, the evaluation of the effects of the TGR on

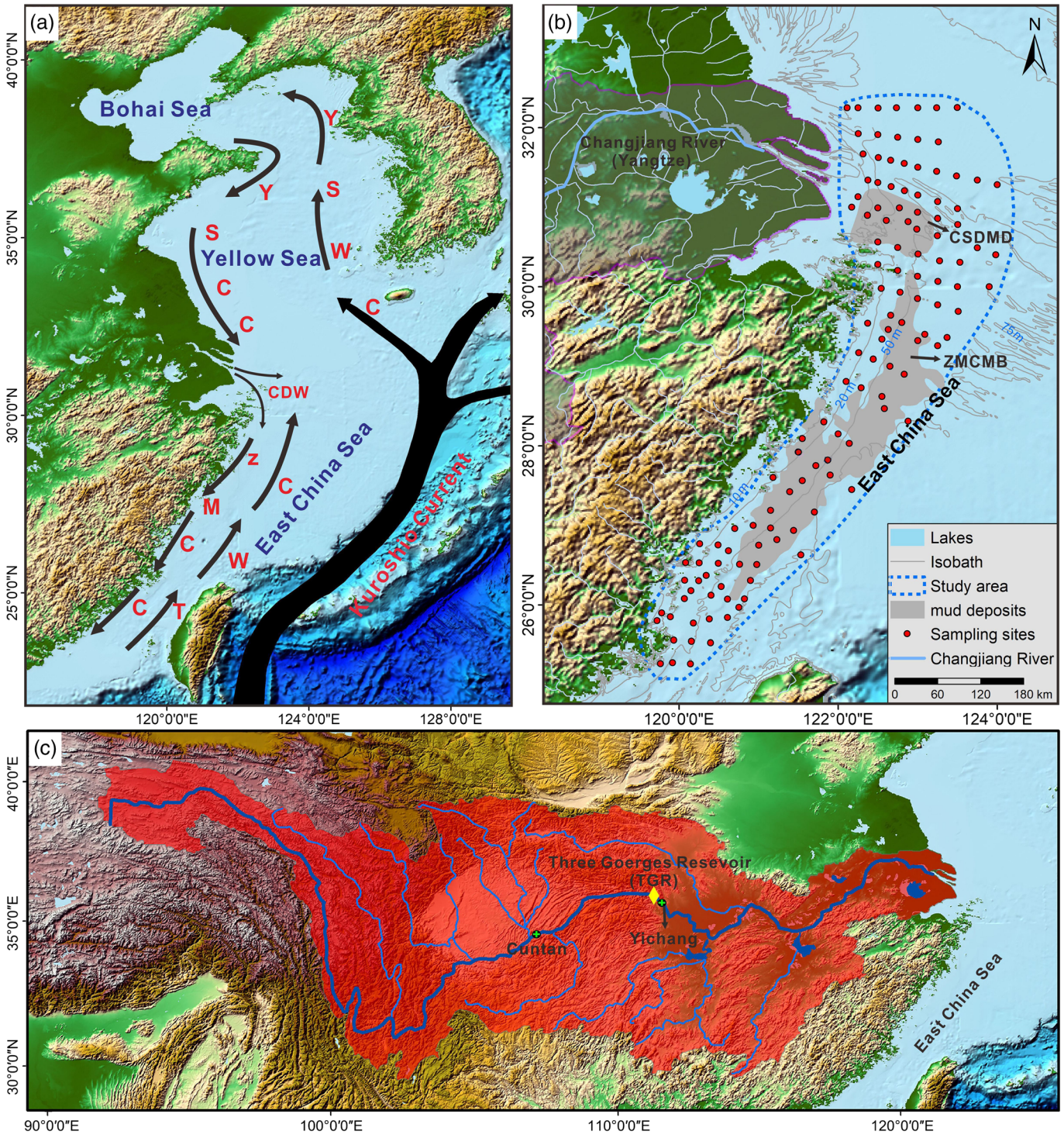


Figure 1. Study area within the East China Sea showing (a) major oceanic currents including the Changjiang-diluted water (CDW), Zhe-Min coastal current (ZMCC), Taiwan warm current (TWC), Yellow Sea coastal current (YSCC), Yellow Sea warm current (YSWC), and Kuroshio current; (b) sampling sites in the estuarine-inner shelf areas of the ECS. The blue dotted line represents the delineations of the study area. Gray patches are mud deposits, namely, the Changjiang Subaqueous Delta mud deposit (CSDMD) and the Zhe-Min Coastal Mud Belts (ZMCMB); and (c) Changjiang (Yangtze) River catchment, ✤ is a hydrologic station, ♦ is the Three Gorges Reservoir (TGR).

19448007, 2020, 17, Downloaded from https://agupubs.onlinelibrary.wiley.com/doi/10.1029/2020GL087357 by Nanjing University, Wiley Online Library on [07/06/2024]. See the Terms and Conditions (https://onlinelibrary.wiley.com/terms-and-conditions) on Wiley Online Library for rules of use; OA articles are governed by the applicable Creative Commons License

19448007, 2020, 17, Downloaded from https://agupubs.onlinelibrary.wiley.com/doi/10.1029/2020GL087357 by Nanjing University, Wiley Online Library on [07/06/2024]. See the Terms and Conditions (https://onlinelibrary.wiley.com/terms-and-conditions) on Wiley Online Library for rules of use; OA articles are governed by the applicable Creative Commons License

these processes remains insufficient. Therefore, the current status of OC burial in the ECS cannot be accurately determined based on previous studies. Herein, we attempted to re-evaluate the transport and burial of OC in the ECS.

Before 2003, few studies were carried out on sedimentary OC in the ECS; therefore, it is difficult to find relevant systematic data. However, previous studies suggest that the responses of the sedimentary environment in the ECS lag behind the catchment changes (Dai et al., 2014), and the residence time of the sediment, recorded from the time of entering the ECS to the deposition on the seabed, is ~2–3 years (Gao et al., 2017; Li et al., 2014; Nozaki et al., 1991). Therefore, the surficial sediments collected in 2006 should exhibit characteristics consistent with the ECS prior to 2003.

In this study, sediment grain size, bulk OC properties, and molecular biomarker data from 2006 were collected from published literature to identify the sedimentary environment and OC distribution in the estuarine-inner shelf region of the ECS before the TGR. To explore the effect of the TGR, we also collected surficial sediments in 2018, spanning from the estuary, along the Zhejiang-Fujian coast to the edge of the ZMCMB (Figure 1b). The OC characteristics collected in 2006 and 2018 were compared to explore the variations in the distribution and deposition of OC in the ECS before versus after the impoundment of the TGR.

2. Methods

2.1. Sampling

In total, 118 surficial sediments (0–2 cm) were collected from the estuarine-inner shelf areas of the ECS using a box corer during cruises on the R/Vs *Xiangyanghong 18* and *Kexue 3* in May 2018. More than 50% of sampling sites were located in the mud deposit. All samples were frozen and stored at −20°C prior to analysis.

2.2. Analytical Procedure

For the analysis of the TOC and its stable isotope, we followed methods described by Xing et al. (2011) and Hu et al. (2012). Briefly, freeze-dried and homogenized samples were decalcified with 4 N HCl for 24 hr. The samples were then repeatedly rinsed with deionized water to neutralize them. A Thermo Flash 2000 Elemental Analyzer interfaced with a MAT-253 isotope ratio mass spectrometer was used to determine the TOC and its stable isotope. The *n*-alkanes were extracted following Hu et al. (2006, 2009), which entailed three sequential ultrasonic extractions with methanol, three extractions with a 1:1 v/v mixture of dichloromethane and methanol, and three extractions with dichloromethane. The *n*-alkanes were identified and quantified using a HP 6890 gas chromatograph with a flame ionization detector. Detailed descriptions of the analytical procedures are provided in Text S1.

2.3. Data Collection

The sediment grain sizes ($n = 141$), bulk OC properties ($n = 131$, TOC, C/N ratios, and $\delta^{13}C$ values), and *n*-alkane contents ($n = 119$) of the 2006 samples were obtained from previous publications (Hu et al., 2012; Xing et al., 2011; Yao et al., 2015). The sampling is described in detail in Text S2. Sedimentation rates were reported by Wang et al. (2017) and Gao et al. (2019). To ensure the comparability of the sedimentation rates, we deliberately selected data obtained with the same dating method, the ^{210}Pb dating method, described in detail in Text S3. The method used to calculate the deposition flux is taken from Wang et al. (2016) and is briefly described in Text S4.

2.4. Statistical Analyses

The significance of the differences in the sediment grain sizes, components, bulk OC properties, and biomarker properties for the two time nodes was tested using ANOVA at a confidence level of 0.01. Additionally, a Pearson correlation matrix was created using the OC characteristics and sediment grain sizes from each station. All statistical calculations were carried out using SPSS version 22.0 (SPSS Institute, USA).

3. Results and Discussion

3.1. Variations in the Bulk OC Characteristics Across the ECS

The variations in the bulk OC characteristics in the estuarine-inner shelf areas of the ECS before versus after the impoundment of the TGR are shown in Figures S2a and S2d and described in detail in Text S5. The TOC content ranged from 0.17% to 0.84% before the TGR, with an average value of 0.56 ± 0.16%, and then

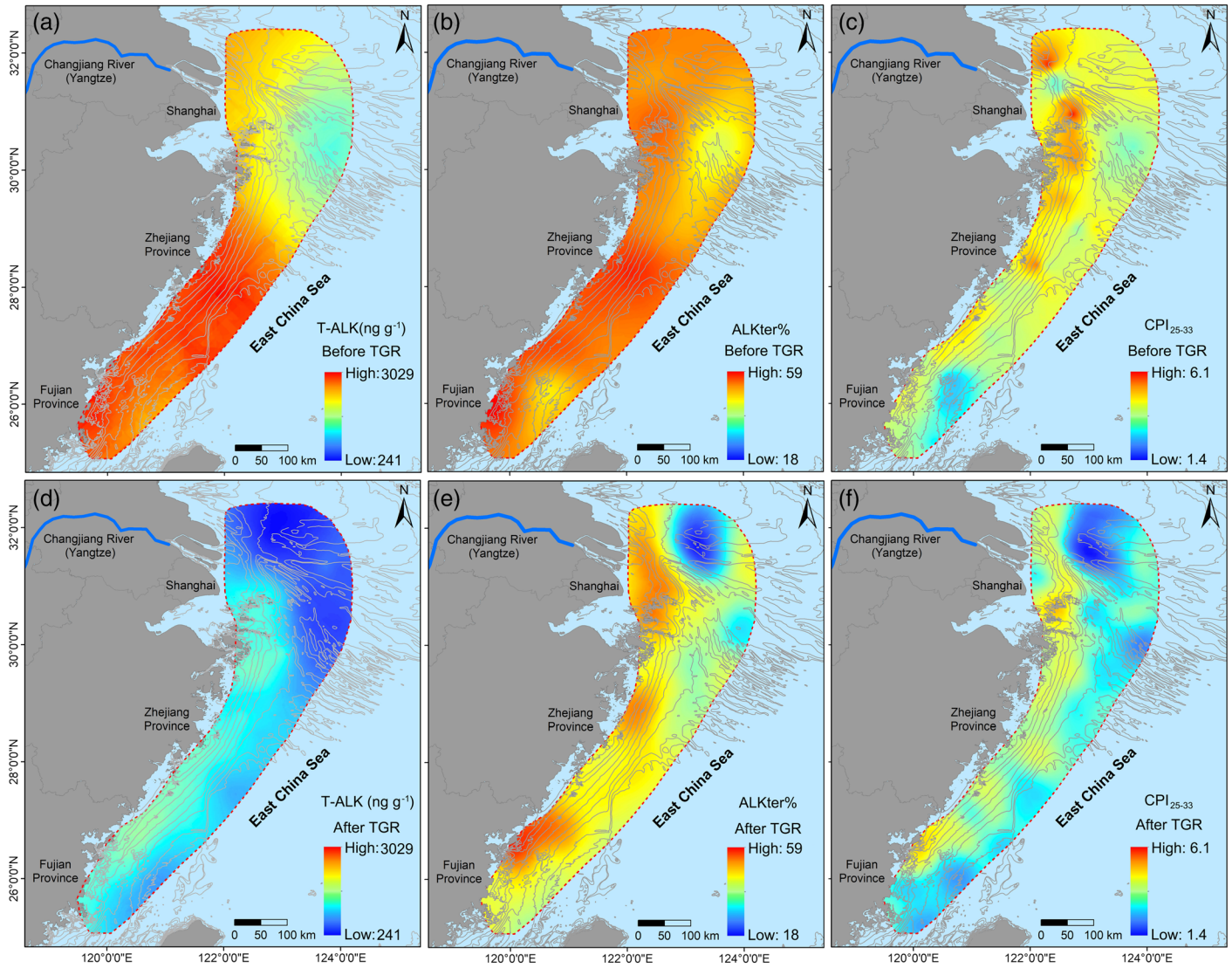


Figure 2. Distributions of molecular biomarkers in surficial sediments from the estuarine-inner shelf areas of the ECS before (upper row) and after (lower row) the impoundment of TGR; (a, d) T-ALK content, (b, e) ALKter%, and (c, f) $CPI_{25–33}$.

decreased to an average of 0.45 ± 0.18%, with a range of 0.11–0.81%, after the TGR. The TOC content in the estuary decreased slightly in the CSDMD ($F = 9.15$, $p = 0.002$), while a drastic decrease was observed east of 123°E ($F = 62.93$, $p < 0.001$). The spatial patterns of the TOC content in the entire ZMCMB exhibited a consistent decreasing trend after the TGR ($F = 51.45$, $p < 0.001$). The distributions of the C/N ratios in the surficial sediments varied between 2006 and 2018 (Figures S2b and S2e) and notably decreased north of 27°N ($F = 319.31$, $p < 0.001$). Similarly, the spatial patterns of $\delta^{13}C$ of the surficial sediments before and after the TGR differed significantly ($F = 7.59$, $p = 0.006$). The $\delta^{13}C$ of the sediments from the CSDMD and adjacent nearshore areas exhibited a declining trend after the TGR impoundment, while the $\delta^{13}C$ values obtained for the offshore region displayed an increasing trend (Figures S2c and S2f).

There was also a significant difference in the distributions of the *n*-alkanes in the surficial sediments from the study area before versus after the impoundment of the TGR (Figure 2). The concentrations of $C_{14–35}$ *n*-alkanes (T-ALK) in the surficial sediments ranged 436–4,312 ng g^{-1} before the TGR, with an average value of 2,502 ± 824 ng g^{-1}, and then significantly decreased to an average of 468 ± 266 ng g^{-1} ($F = 631.09$, $p < 0.001$), with a range of 33–1,661 ng g^{-1} after the TGR (Figures 2a and 2d). The reduction of the terrestrial input, which primarily originates from leaf wax in terrestrial higher plants, could be the main reason for the

19448007, 2020, 17, Downloaded from https://agupubs.onlinelibrary.wiley.com/doi/10.1029/2020GL087357 by Nanjing University, Wiley Online Library on [07/06/2024]. See the Terms and Conditions (https://onlinelibrary.wiley.com/terms-and-conditions) on Wiley Online Library for rules of use; OA articles are governed by the applicable Creative Commons License

19448007, 2020, 17, Downloaded from https://agupubs.onlinelibrary.wiley.com/doi/10.1029/2020GL087357 by Nanjing University, Wiley Online Library on [07/06/2024]. See the Terms and Conditions (https://onlinelibrary.wiley.com/terms-and-conditions) on Wiley Online Library for rules of use; OA articles are governed by the applicable Creative Commons License

larger decrease in T-ALK compared with the TOC content (Eglinton & Hamilton, 1967). The *n*-alkanes in sediment are dominated by odd-numbered homologues, with the C_{27}, C_{29}, C_{31}, and C_{33} *n*-alkanes, indicative of terrestrial OC (Feng et al., 2013; Yunker et al., 2005), are the most abundant. The sum of these four homologues is referred to as "terrigenous *n*-alkanes" (ALKter), and the percentage of ALKter in T-ALK (ALKter%) can be used to indicate the contribution of terrestrial OC (Hu et al., 2012). In this study, the ALKter% of the surficial sediments ranged from 20% to 68% before the TGR impoundment, with a mean value of 51 ± 10% (Figure 2b), illustrating the terrestrial OC dominance of sedimentary OC in the study area. The mean ALKter% of the surficial sediments decreased to 43 ± 13% after the TGR impoundment, with a range of 4.6–70% (Figure 2e). This indicates that the proportion of terrestrial OC at most locations decreased after the TGR impoundment.

Variations in the ALKter% located offshore at water depths >50 m were more significant than the variations determined for sediments from the shallow nearshore region ($F = 179.65$, $p < 0.001$; Figures 2b and 2e). The high molecular weight carbon preference index ($CPI_{25-33} = (1/2)$ (ΣC_{25-33} odd-numbered *n*-alkanes/ΣC_{24-32} even-numbered *n*-alkanes) + (1/2) (ΣC_{25-33} odd-numbered *n*-alkanes/ΣC_{26-34} even-numbered *n*-alkanes)) is generally used to identify the degradation of terrestrial OC. In this study, the CPI_{25-33} of the surficial sediments exhibited a uniform spatial pattern before the TGR; it ranged from 2.6 to 6.1, with a mean value of 4.2 ± 0.8 (Figure 2c). This range is comparable to the value reported for extant living plants ($CPI_{25-33} > 5$; Vonk et al., 2010). After the TGR, the mean CPI_{25-33} in the surficial sediments drastically decreased to 3.3 ± 0.9 ($F = 69.15$, $p < 0.001$), with a range of 1.1–5.5 (Figure 2f). The variations in the CPI_{25-33} of the sediments indicate that the degradation of sedimentary OC in the study area intensified after the TGR, especially in the offshore region at depths above 50 m (Figures 2c and 2f).

3.2. Response of Sedimentary OC to Riverine Input and Hydrodynamic Processes

The distributions, compositions, and contents of sedimentary OC in the study area before and after the TGR impoundment vary significantly. The TGR intercepted large amounts of sediment from upstream sections, which inevitably reduced the POC flux discharged into the ECS. Based on the POC fluxes recorded at the hydrologic stations upstream (Cuntan Station, located at the head of the fluctuating backwater zone of the TGR) and downstream (Yichang Station, located 3 km downstream of the TGR) of the TGR (Figures 1c and S3), we roughly estimated that the POC interception of the TGR was ~2.13 Mt yr^{-1} (Figure S3), which was consistent with the interception rate of ~2.10 Mt yr^{-1} obtained by Li et al. (2015). Therefore, the calculated interception efficiency reached up to 84%, suggesting that the TGR plays a crucial role in trapping POC from the upstream of the Changjiang River. The reduction of the POC flux could be the main reason for the variations in the distribution and content of the sedimentary OC in the ECS.

While the variations in the sedimentary OC can be partly attributed to the reduction in the terrestrial POC input, the hydrodynamic process is also considered a factor affecting the fate of sedimentary OC in marginal seas (Bao et al., 2018, 2019; Bianchi et al., 2018; Bröder et al., 2016, 2018). We have confirmed that the sedimentary environment in the study area changed due to the sharp reduction in the sediment load (Wang, Hao, Feng, Zhang, Li, et al., 2020), which would inevitably affect the dispersal and burial of POC. The sediment flux discharged from the Changjiang River to the ECS dropped from 340 Mt yr^{-1} in 1986–2002 to 145 Mt yr^{-1} after the TGR impoundment, which is insufficient to maintain the geomorphic stability of the CSDMD (Yang et al., 2018). Therefore, the seabed sediment in the CSDMD was eroded and transported southward by coastal currents. Long periods of insufficient sediment supply have caused erosion to spread further into the ZMCMB (Gao et al., 2019; Wang, Hao, Feng, Zhang, Li, et al., 2020). Large amounts of fine-grained particles in the seabed sediment have been washed away, which has significantly changed the sediment grain sizes and components in the study area.

The mean grain size of the surficial sediments obtained in 2006 ranged from 2.5 to 7.3 Φ ($\Phi = -\log_2 D$, where D is the sediment grain size in mm), with an average value of 6.4 ± 1.2 Φ (Figure S4a). This is slightly coarser than the average value of 6.7 ± 0.2 Φ obtained in 1982 (Gao et al., 2019). The variations in the grain size of the surficial sediment between 1982 and 2006 can be ignored, as 0.5 Φ has been suggested as the threshold value for filtering out seasonal and spring-neap tidal effects (Yang et al., 2018). Therefore, although the TGR impoundment began in 2003, the sedimentary environment in the study area remained stable until 2006. Thereafter, the grain size of the surficial sediment decreased to 4.4 ± 2.1 Φ in 2018 (F = 220.46,

19448007, 2020, 17, Downloaded from https://agupubs.onlinelibrary.wiley.com/doi/10.1029/2020GL087357 by Nanjing University, Wiley Online Library on [07/06/2024]. See the Terms and Conditions (https://onlinelibrary.wiley.com/terms-and-conditions) on Wiley Online Library for rules of use; OA articles are governed by the applicable Creative Commons License

$p < 0.001$), likely because of the enhanced seabed erosion in the study area caused by the sharp decline in the sediment load. After the TGR, the mean clay and sand component contents of the surficial sediments drastically decreased and increased, respectively ($F = 5140.78$, $p < 0.001$; $F = 220.66$, $p < 0.001$; Figures S4b and S4f and S4d and S4h), while the mean content of the silt component changed slightly ($F = 9.16$, $p < 0.002$; Figures S4c and S4g). The sharp reduction in the clay component illustrated that seabed erosion scoured large amounts of fine-grained components from the surficial sediments. The variations in the spatial pattern of the silt component indicated that a portion of the silt that was originally deposited in the estuary was eroded, transported southward, and eventually deposited in the ZMCMB (Figures S4c and S4g). The sharp variations in the spatial patterns of the sediment grain sizes and components illustrated that seabed erosion resulted in enhanced sediment mobilization.

Previous studies suggest that OC preservation in the sediments of marginal seas can be attributed mainly to physical protection via mineral associations (Arnarson & Keil, 2007; Burdige, 2005, 2007). Fine-grained particles with large specific surface areas are considered to be the main particles OC adheres to (Burdige, 2007; Mayer, 1994; Mayer et al., 2004). This suggests that the transport and redistribution of seabed sediments inevitably affected the burial of OC in the study area. Our results indicated significant positive correlations between the OC characteristics and the clay and silt components (Table S1). In other words, larger amounts of fine-grained sediment corresponded to higher TOC and T-ALK contents. Thus, the reduction in the clay content could be another main reason for the direct reduction in the TOC content in the study area after the TGR.

The sortable silt fraction (3–8 Φ) defined by McCave and Hall (2006) is considered to have the greatest potential to be eroded and remobilized, which plays an important role in controlling the fate of the sedimentary OC in the study area (Bao et al., 2016, 2018). Seabed erosion and sediment remobilization processes can lead to multiple resuspension-deposition loops of OC associated with fine-grained sediments during southward transport. This prolongs the oxygen exposure and transport duration and further promotes the lateral redistribution and degradation of OC (Blair & Aller, 2012; Bröder et al., 2018). Therefore, the variations in the distribution of the silt fraction could be an important factor in the transport and burial of OC in the study area. In addition, changes in marine production could be another potential process affecting the distribution and transport of sedimentary OC in the ECS and thus should be researched further.

3.3. Re-Evaluating the Potential of OC Deposition in the ECS and its Global Implications

The above-mentioned results indicated that reduced riverine input seriously influenced the distribution and transport of OC in the study area, which could inevitably change the OC burial. Here, we attempted to re-evaluate the potential for OC deposition in this area by comparing the OC deposition fluxes before versus after the TGR impoundment. The sedimentation rate for the study area before and after the TGR were collected and interpolated to acquire the spatial patterns (Figures S5a and S5b). The sedimentation rate in the study area before the TGR ranged from 0.1 to 6.3 cm yr^{-1}, with a mean value of 1.38 ± 1.30 cm yr^{-1}, which drastically decreased to an average of 0.63 ± 0.34 cm yr^{-1} after the TGR, with a range of 0.16–1.75 cm yr^{-1}. The spatial pattern of the sedimentation rate also changed; it became relatively uniform and the depocenter disappeared (Figures S5a and S5b). Such variations also confirm the aforementioned results, which indicated that seabed erosion occurred in the study area, especially in the CSDMD.

Based on the sedimentation rates and TOC contents, we approximated the deposition flux of OC in the study area. The deposition flux of OC before the TGR ranged 0.10–1.60 g m^{-2} yr^{-1}, with a mean value of 1.20 ± 1.60 g m^{-2} yr^{-1} (Figure 3a). The distribution pattern of the TOC flux before the TGR was similar to that of the sedimentation rate, with a high OC deposition flux in the CSDMD, followed by that in the ZMCMB. After the TGR impoundment, the average OC deposition flux in the study area sharply decreased to 0.10 ± 0.05 g m^{-2} yr^{-1} ($F = 552.27$, $p < 0.001$), with a range of 0.09–0.15 g m^{-2} yr^{-1} (Figure 3b). The spatial pattern of the OC deposition flux also significantly changed and became relatively uniform throughout the region (Figure 3b).

To obtain a better understanding of the differences in the OC deposition flux before versus after the impoundment of the TGR, correlation analyses were carried out to examine the relationships between the deposition flux and sedimentation rate/TOC content. The results are shown in Figure S6. Before the TGR, the deposition flux was weakly correlated with the TOC content (Figure S6b) and strongly correlated with the sedimentation rate (Figure S6a). In contrast, after the TGR impoundment, the deposition flux was strongly correlated with

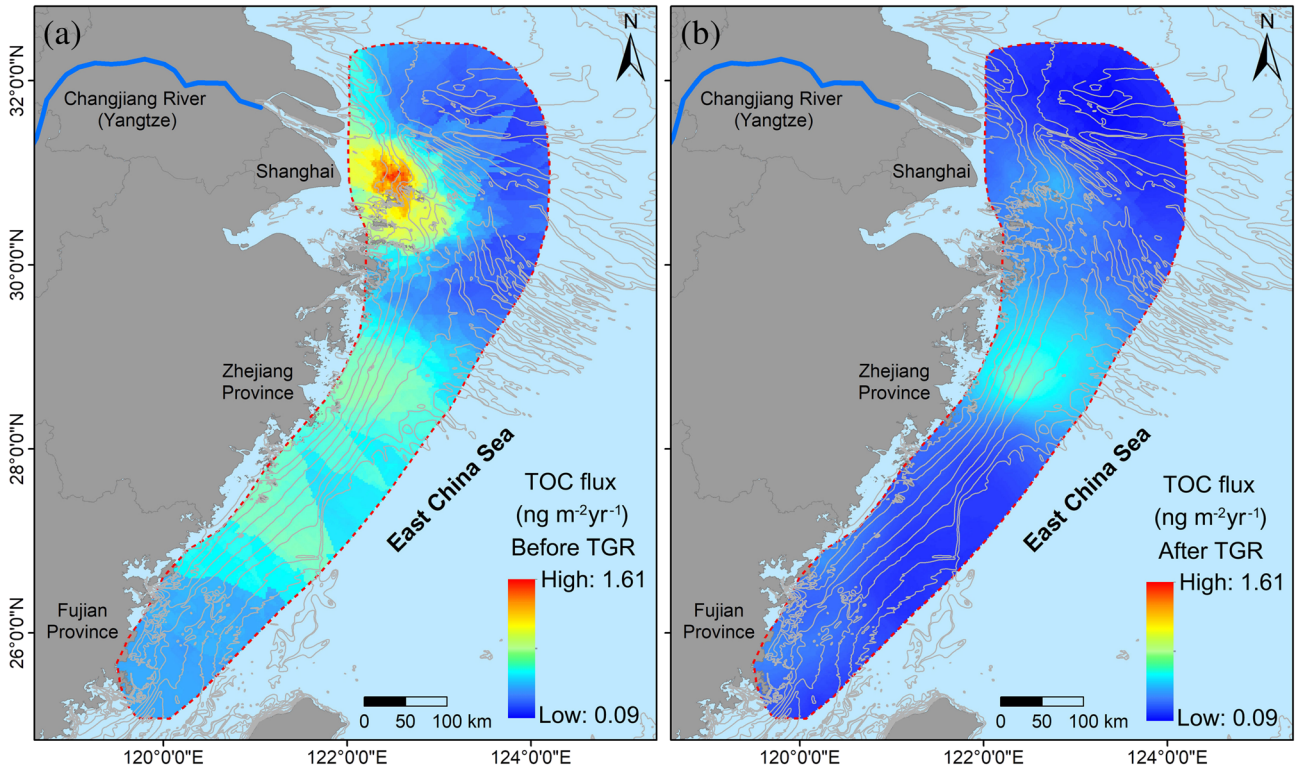


Figure 3. Deposition fluxes of OC in the estuarine–inner shelf areas of the ECS (a) before and (b) after the impoundment of the TGR.

the TOC content (Figure S6d) and weakly correlated with the sedimentation rate (Figure S6c). Therefore, the effect of the sedimentation rate on the OC deposition flux gradually weakened due to seabed erosion after the TGR impoundment. Finally, we estimated an OC deposition flux of ~1.28×10^5 km^2 in the study area for ~6.13 Mt yr^{-1} before the TGR, which dropped to 3.21 Mt yr^{-1} afterwards (Figure 4). The OC deposition flux decreased by ~48% after the TGR impoundment, mainly due to the decreased sedimentation rate and TOC content. Therefore, intense anthropogenic perturbations in the Changjiang River-ECS sedimentary system seriously affected the OC burial potential in the study area.

The contributions of terrestrial and marine OC were also estimated to better understand such large reductions in the OC deposition flux in the study area (Text S6). Marine OC accounted for 72% and 78% of the total OC deposition fluxes before and after the TGR, respectively. The study area was divided into two subregions, that is, the estuary and inner shelf area, with 30°N as the dividing line. Following the TGR impoundment, the deposition fluxes of marine and terrestrial OC in the estuary decreased by ~49% and ~63%, respectively, while deposition fluxes of marine and terrestrial OC in the inner shelf area decreased by 40% and 56%, respectively. Therefore, the OC deposition flux in the estuary exhibited a more drastic decline than that of the inner shelf area, and both the terrestrial and marine OC deposition fluxes decreased sharply. After the TGR impoundment, the OC deposition flux in the estuary and inner shelf area decreased by 1.33 and 1.63 Mt, respectively (Figure 4). We infer that the seabed erosion may have been the main factor leading to the reduction of the marine OC deposition flux.

While our results show anthropogenic perturbations of carbon deposition in the ECS, these variations are not restricted to this region. Such variations are likely to be found in other river-dominated passive margins due to their broad continental shelves. The magnitudes of the variations will depend on the intensity of human activity, sediment composition, and regional hydrodynamic and geomorphic characteristics. Over the past half century, many rivers, including the Indus, Ganges-Bangladesh, Irrawaddy, Mekong, Mississippi, Pearl, and Yellow River, have experienced drastically reduced sediment loads (Milliman, 1997; Rahman et al., 2018; Syvitski et al., 2009; Wang et al., 2015). Such reductions in the sediment loads have triggered erosion of estuarine shoals and subaqueous deltas (Anthony et al., 2015; Blum & Roberts, 2009; Stanley, 1996). For instance, the

19448007, 2020, 17, Downloaded from https://agupubs.onlinelibrary.wiley.com/doi/10.1029/2020GL087357 by Nanjing University, Wiley Online Library on [07/06/2024]. See the Terms and Conditions (https://onlinelibrary.wiley.com/terms-and-conditions) on Wiley Online Library for rules of use; OA articles are governed by the applicable Creative Commons License

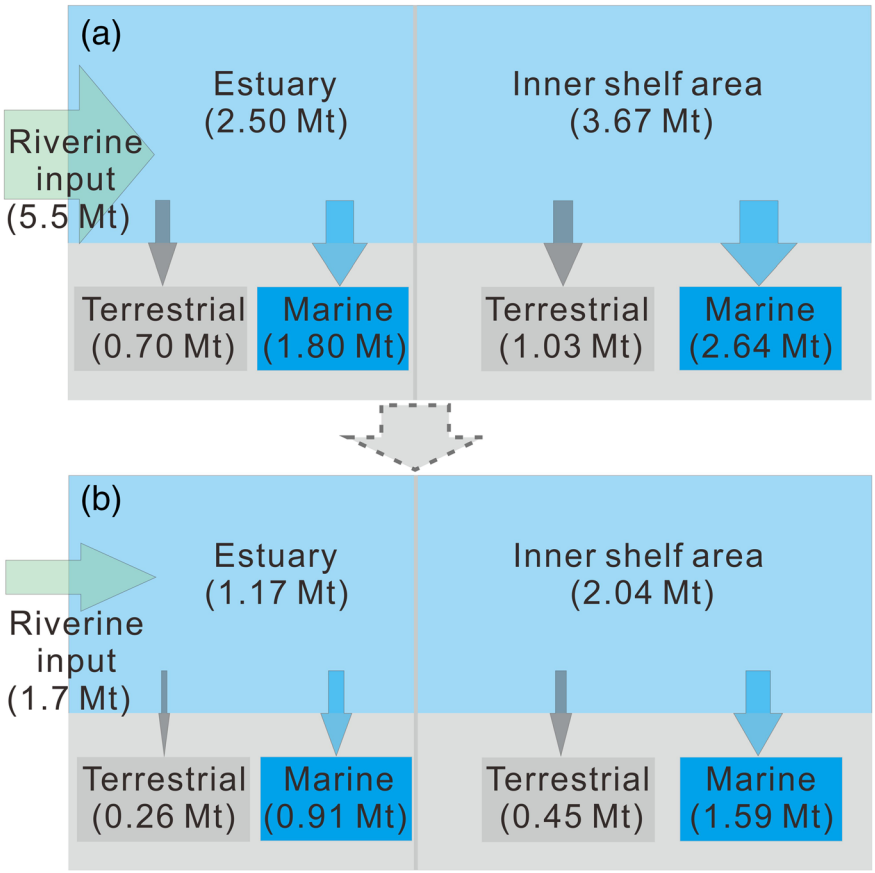


Figure 4. Burial patterns of OC in the estuarine-inner shelf areas of the ECS (a) before and (b) after the impoundment of the TGR.

retrogradation of the subaqueous delta of the Mississippi River has begun due to dam construction (Maloney et al., 2018). The transformation of deltas or continental shelves from accretion to erosion inevitably triggers sediment (re)mobilization and the scouring of OC associated with fine-grained sediments. Such processes may have greater effects on passive margins that host broad continental shelves, resulting in prolonged oxygen exposure during resuspension-deposition loops. This may in turn promote the lateral redistribution and degradation of OC (Bao et al., 2018; Blair & Aller, 2012). Therefore, the effect of reduced riverine input, coupled with the impact of seabed erosion and OC degradation during sediment (re)mobilization, may lead to a significant decrease in the OC deposition fluxes at passive continental shelves. Accordingly, further studies should be carried out to examine the effects of intense anthropogenic perturbations on OC burial in river-dominated passive margins at global scales.

Data Availability Statement

We have archived our data in an appropriate repository, which are available at https://zenodo.org/record/3825961#.Xryx36czaCo.

Acknowledgments

The study was supported by the Marine Science and Technology Innovation Project of Jiangsu Province (HY2018-9) and the National Science Foundation of China (Grants 41601560, 41471431, and 41776048).

References

Anthony, E., Brunier, G., Besset, M., Goichot, M., Dussouillez, P., & Nguyen, V. L. (2015). Linking rapid erosion of the Mekong River Delta to human activities. *Scientific Reports*, *5*(1), 14745. https://doi.org/10.1038/srep14745

Arnarson, T. S., & Keil, R. G. (2007). Changes in organic matter-mineral interactions for marine sediments with varying oxygen exposure times. *Geochimica et Cosmochimica Acta*, *71*(14), 3545–3556. https://doi.org/10.1016/j.gca.2007.04.027

Bao, R., Blattmann, T. M., McIntyre, C., Zhao, M., & Eglinton, T. I. (2019). Relationships between grain size and organic carbon ^{14}C heterogeneity in continental margin sediments. *Earth and Planetary Science Letters*, *505*, 76–85. https://doi.org/10.1016/j.epsl.2018.10.013

19448007, 2020, 17, Downloaded from https://agupubs.onlinelibrary.wiley.com/doi/10.1029/2020GL087357 by Nanjing University, Wiley Online Library on [07/06/2024]. See the Terms and Conditions (https://onlinelibrary.wiley.com/terms-and-conditions) on Wiley Online Library for rules of use; OA articles are governed by the applicable Creative Commons License

Bao, R., McIntyre, C., Zhao, M., Zhu, C., Kao, S. J., & Eglinton, T. I. (2016). Widespread dispersal and aging of organic carbon in shallow marginal seas. *Geology*, *44*(10), 791–794. https://doi.org/10.1130/G37948.1

Bao, R., van der Voort, T. S., Zhao, M., Guo, X., Montluçon, D. B., McIntyre, C., & Eglinton, T. I. (2018). Influence of hydrodynamic processes on the fate of sedimentary organic matter on continental margins. *Global Biogeochemical Cycles*, *32*(9), 1420–1432. https://doi.org/10.1029/2018GB005921

Bianchi, T., Cui, X., Blair, N. E., Burdige, D. J., Eglinton, T. I., & Galy, V. (2018). Centers of organic carbon burial and oxidation at the land-ocean interface. *Organic Geochemistry*, *115*, 138–155. https://doi.org/10.1016/j.orggeochem.2017.09.008

Bianchi, T. S., & Allison, M. A. (2009). Large-river delta-front estuaries as natural "recorders" of global environmental change. *Proceedings of the National Academy of Sciences*, *106*(20), 8085–8092. https://doi.org/10.1073/pnas.0812878106

Blair, N. E., & Aller, R. C. (2012). The fate of terrestrial organic carbon in the marine environment. *Annual Review of Marine Science*, *4*(1), 401–423. https://doi.org/10.1146/annurev-marine-120709-142717

Blum, M. D., & Roberts, H. H. (2009). Drowning of the Mississippi Delta due to insufficient sediment supply and global sea-level rise. *Nature Geoscience*, *2*(7), 488–491. https://doi.org/10.1038/ngeo553

Bröder, L., Tesi, T., Andersson, A., Semiletov, I., & Gustafsson, Ö. (2018). Bounding cross-shelf transport time and degradation in Siberian-Arctic land-ocean carbon transfer. *Nature Communications*, *9*(1), 806. https://doi.org/10.1038/s41467-018-03192-1

Bröder, L., Tesi, T., Salvadó, J. A., Semiletov, I. P., Dudarev, O. V., & Gustafsson, Ö. (2016). Fate of terrigenous organic matter across the Laptev Sea from the mouth of the Lena River to the deep sea of the Arctic interior. *Biogeosciences*, *13*(17), 5003–5019. https://doi.org/10.5194/bg-13-5003-2016

Burdige, D. J. (2005). Burial of terrestrial organic matter in marine sediments: A re-assessment. *Global Biogeochemical Cycles*, *19*, GB4011. https://doi.org/10.1029/2004GB002368

Burdige, D. J. (2007). Preservation of organic matter in marine sediments: Controls, mechanisms, and an imbalance in sediment organic carbon budgets? *Chemical Reviews*, *107*(2), 467–485. https://doi.org/10.1021/cr050347q

Dai, Z. J., Liu, J. T., Wei, W., & Chen, J. Y. (2014). Detection of the Three Gorges Dam influence on the Changjiang (Yangtze River) submerged delta. *Science Reports*, *2014*(4), 6600.

Deng, B., Zhang, J., & Wu, Y. (2006). Recent sediment accumulation and carbon burial in the East China Sea. *Global Biogeochemical Cycles*, *20*, GB3014. https://doi.org/10.1029/2005GB002559

Eglinton, G., & Hamilton, R. J. (1967). Leaf epicuticular waxes. *Science*, *156*(3780), 1322–1335. https://doi.org/10.1126/science.156.3780.1322

Feng, X., Vonk, J. E., van Dongen, B. E., Gustafsson, O., Semiletov, I. P., Dudarev, O. V., et al. (2013). Differential mobilization of terrestrial carbon pools in Eurasian Arctic river basins. *Proceedings of the National Academy of Sciences*, *110*(35), 14,168–14,173. https://doi.org/10.1073/pnas.1307031110

Galy, V., Peucker-Ehrenbrink, B., & Eglinton, T. (2015). Global carbon export from the terrestrial biosphere controlled by erosion. *Nature*, *521*(7551), 204–207. https://doi.org/10.1038/nature14400

Gao, J., Jia, J., Sheng, H., Yu, R., Li, G. C., Wang, Y. P., et al. (2017). Variations in the transport, distribution and budget of ^{210}Pb in sediment over the estuarine and inner shelf areas of the East China Sea due to Changjiang catchment changes. *Journal of Geophysical Research: Earth Surface*, *122*, 235–247. https://doi.org/10.1002/2016JF004130

Gao, J., Shi, Y., Sheng, H., Kettner, A. J., Yang, Y., Jia, J. J., et al. (2019). Rapid response of the Changjiang (Yangtze) River and East China Sea source-to-sink conveying system to human induced catchment perturbations. *Marine Geology*, *414*, 1–17. https://doi.org/10.1016/j.margeo.2019.05.003

Gao, S., & Collins, M. B. (2014). Holocene sedimentary systems on continental shelves. *Marine Geology*, *352*, 268–294. https://doi.org/10.1016/j.margeo.2014.03.021

Hu, J., Peng, P. A., & Chivas, A. R. (2009). Molecular biomarker evidence of origins and transport of organic matter in sediments of the Pearl River estuary and adjacent South China Sea. *Applied Geochemistry*, *24*(9), 1666–1676. https://doi.org/10.1016/j.apgeochem.2009.04.035

Hu, J., Zhang, H., & Peng, P. A. (2006). Fatty acid composition of surface sediments in the subtropical Pearl River estuary and adjacent shelf, Southern China. *Estuarine, Coastal and Shelf Science*, *66*(1–2), 346–356. https://doi.org/10.1016/j.ecss.2005.09.009

Hu, L., Shi, X., Yu, Z., Lin, T., Wang, H., Ma, D., et al. (2012). Distribution of sedimentary organic matter in estuarine-inner shelf regions of the East China Sea: Implications for hydrodynamic forces and anthropogenic impact. *Marine Chemistry*, *142*, 29–40.

Kao, S. J., Lin, F. J., & Liu, K. K. (2003). Organic carbon and nitrogen contents and their isotopic compositions in surficial sediments from the East China Sea shelf and the southern Okinawa Trough. Deep Sea Research. *Part II: Topical Studies in Oceanography*, *50*(6–7), 1203–1217.

Li, D., Yao, P., Bianchi, T. S., Zhang, T., Zhao, B., Pan, H., et al. (2014). Organic carbon cycling in sediments of the Changjiang Estuary and adjacent shelf: Implication for the influence of Three Gorges Dam. *Journal of Marine Systems*, *139*, 409–419. https://doi.org/10.1016/j.jmarsys.2014.08.009

Li, G., Wang, X. T., Yang, Z., Mao, C., West, A. J., & Ji, J. (2015). Dam-triggered organic carbon sequestration makes the Changjiang (Yangtze) River basin (China) a significant carbon sink. *Journal of Geophysical Research: Biogeosciences*, *120*, 39–53. https://doi.org/10.1002/2014JG002646

Liu, J. P., Xu, K. H., Li, A. C., Milliman, J. D., Velozzi, D. M., Xiao, S. B., & Yang, Z. S. (2007). Flux and fate of Yangtze River sediment delivered to the East China Sea. *Geomorphology*, *85*(3–4), 208–224. https://doi.org/10.1016/j.geomorph.2006.03.023

Ludwig, W., & Probst, J. L. (1998). River sediment discharge to the oceans; present-day controls and global budgets. *American Journal of Science*, *298*(4), 265–295. https://doi.org/10.2475/ajs.298.4.265

Maloney, J., Bentley, S. J., Xu, K., Obelcz, J., Georgiou, I. Y., & Miner, M. D. (2018). Mississippi river subaqueous delta is entering a stage of retrogradation. *Marine Geology*, *400*, 12–23. https://doi.org/10.1016/j.margeo.2018.03.001

Mayer, L. M. (1994). Surface area control of organic carbon accumulation in continental shelf sediments. *Geochimica et Cosmochimica Acta*, *58*(4), 1271–1284. https://doi.org/10.1016/0016-7037(94)90381-6

Mayer, L. M., Schick, L. L., Hardy, K. R., Wagai, R., & Mccarthy, J. (2004). Organic matter in small mesopores in sediments and soils. *Geochimica et Cosmochimica Acta*, *68*(19), 3863–3872. https://doi.org/10.1016/j.gca.2004.03.019

McCave, I., & Hall, I. (2006). Size sorting in marine muds: Processes, pitfalls, and prospects for paleoflow-speed proxies. *Geochemistry, Geophysics, Geosystems*, *7*, Q10N05. https://doi.org/10.1029/2006GC001284

Milliman, J. D. (1997). Blessed dams or damned dams? *Nature*, *386*(6623), 325–327. https://doi.org/10.1038/386325a0

Milliman, J. D., & Farnsworth, K. L. (2011). *River discharge to the coastal ocean: A global synthesis*. Press, Cambridge: Cambridge University.

19448007, 2020, 17, Downloaded from https://agupubs.onlinelibrary.wiley.com/doi/10.1029/2020GL087357 by Nanjing University, Wiley Online Library on [07/06/2024]. See the Terms and Conditions (https://onlinelibrary.wiley.com/terms-and-conditions) on Wiley Online Library for rules of use; OA articles are governed by the applicable Creative Commons License

Nozaki, Y., Tsubota, H., Kasemsupaya, V., Yashima, M., & Naoko, I. (1991). Residence times of surface water and particle-reactive ^{210}Pb and ^{210}Po in the East China and Yellow seas. *Geochimica et Cosmochimica Acta*, *55*(5), 1265–1272. https://doi.org/10.1016/0016-7037(91)90305-O

Rahman, M., Dustegir, M., Karim, R., Haque, A., Nicholls, R. J., Darby, S. E., et al. (2018). Recent sediment flux to the Ganges-Brahmaputra-Meghna delta system. *Science of the Total Environment*, *643*, 1054–1064. https://doi.org/10.1016/j.scitotenv.2018.06.147

Raymond, P., McClelland, J. W., Holmes, R. M., Zhulidov, A. V., Mull, K., Peterson, B. J., et al. (2007). Flux and age of dissolved organic carbon exported to the Arctic Ocean: A carbon isotopic study of the five largest arctic rivers. *Global Biogeochemical Cycles*, *21*, GB4011. https://doi.org/10.1029/2007/GB002934

Stanley, D. J. (1996). Nile delta: Extreme case of sediment entrapment on a delta plain and consequent coastal land loss. *Marine Geology*, *129*(3–4), 189–195. https://doi.org/10.1016/0025-3227(96)83344-5

Syvitski, J. P. M., Kettner, A. J., Overeem, I., Hutton, E. W. H., Hannon, M. T., Brakenridge, G. R., et al. (2009). Sinking deltas due to human activities. *Nature Geoscience*, *2*(10), 681–686. https://doi.org/10.1038/ngeo629

Vonk, J., Sánchez-García, L., Semiletov, I. P., Dudarev, O. V., Eglinton, T. I., Andersson, A., & Gustafsson, Ö. (2010). Molecular and radiocarbon constraints on sources and degradation of terrestrial organic carbon along the Kolyma paleoriver transect, East Siberian Sea. *Biogeosciences*, *7*(10), 3153–3166. https://doi.org/10.5194/bg-7-3153-2010

Wang, C., Hao, Z., Feng, Z., Zhang, C., Gao, J., Li, Y., et al. (2020). Rapid changes in organochlorine pesticides in sediments from the East China Sea and their response to human-induced catchment changes. *Water Research*, *169*, 115225. https://doi.org/10.1016/j.watres.2019.115225

Wang, C., Hao, Z., Feng, Z., Zhang, C., Li, Y., Yu, W., & Zou, X. (2020). Shifts in the distribution and fate of sedimentary polycyclic aromatic hydrocarbons within the estuarine-inner shelf areas of the East China Sea: Response to human-induced catchment change. *Journal of Geophysical Research: Oceans*, *125*, e2019JC015773. https://doi.org/10.1029/2019JC015773

Wang, C., Zou, X., Gao, J., Zhao, Y., Yu, W., Li, Y., & Song, Q. (2016). Pollution status of polycyclic aromatic hydrocarbons in surface sediments from the Yangtze River Estuary and its adjacent coastal zone. *Chemosphere*, *162*, 80–90. https://doi.org/10.1016/j.chemosphere.2016.07.075

Wang, C., Zou, X. Q., Zhao, Y. F., Li, Y. L., Song, Q. C., Wang, T., & Yu, W. W. (2017). Distribution pattern and mass budget of sedimentary polycyclic aromatic hydrocarbons in shelf areas of the Eastern China Marginal Seas. *Journal of Geophysical Research: Oceans*, *122*, 4990–5004. https://doi.org/10.1002/2017JC012890

Wang, S., Fu, B., Piao, S., Lü, Y., Ciais, P., Feng, X., & Wang, Y. (2015). Reduced sediment transport in the yellow river due to anthropogenic changes. *Nature Geoscience*, *9*, 38–41.

Wu, Y., Eglinton, T., Yang, L., Deng, B., Montluçon, D., & Zhang, J. (2013). Spatial variability in the abundance, composition, and age of organic matter in surficial sediments of the East China Sea. *Journal of Geophysical Research: Biogeosciences.*, *118*, 1–3.

Xing, L., Zhang, H., Yuan, Z., Sun, Y., & Zhao, M. (2011). Terrestrial and marine biomarker estimates of organic matter sources and distributions in surface sediments from the East China Sea shelf. *Continental Shelf Research.*, *31*(10), 1106–1115. https://doi.org/10.1016/j.csr.2011.04.003

Yang, H. F., Yang, S. L., Xu, K. H., Milliman, J. D., Wang, H., Yang, Z., et al. (2018). Human impacts on sediment in the Yangtze River: A review and new perspectives. *Global Planetary Change*, *162*, 8–17. https://doi.org/10.1016/j.gloplacha.2018.01.001

Yao, P., Yu, Z., Bianchi, T. S., Guo, Z., Zhao, M., Knappy, C. S., et al. (2015). A multiproxy analysis of sedimentary organic carbon in the Changjiang Estuary and adjacent shelf. *Journal of Geophysical Research: Biogeosciences*, *120*, 1407–1429. https://doi.org/10.1002/2014JG002831

Yunker, M. B., Belicka, L. L., Harvey, H. R., & Macdonald, R. W. (2005). Tracing the inputs and fate of marine and terrigenous organic matter in Arctic Ocean sediments: A multivariate analysis of lipid biomarkers. *Deep Sea Research Part II: Topical Studies in Oceanography*, *52*(24–26), 3478–3508. https://doi.org/10.1016/j.dsr2.2005.09.008

19448007, 2020, 17, Downloaded from https://agupubs.onlinelibrary.wiley.com/doi/10.1029/2020GL087357 by Nanjing University, Wiley Online Library on [07/06/2024]. See the Terms and Conditions (https://onlinelibrary.wiley.com/terms-and-conditions) on Wiley Online Library for rules of use; OA articles are governed by the applicable Creative Commons License